Supporting Information

Synergy Strategy to the Flexible Alkyl and Chloride Side-chains Engineered Quinoxaline-Based D-A Conjugated Polymers for Efficient Non-fullerene Polymer Solar Cells

Liang Zeng, ‡[a,c] *Ruijie Ma*, ‡[,b,d] *Qiang Zhang*,[a] *Tao Liu*,*[b,d] *Yiqun Xiao*,[e]

Kai Zhang,[a] *Suqing Cui*,[a] *Weiguo Zhu*,[a] *Xinhui Lu*,[e] *He Yan*,*[b,d,] *Yu Liu**[a,c]

[a] *School of Materials Science and Engineering, Jiangsu Collaboration Innovation*

[a]*Center of Photovoltaic Science and Engineering, Jiangsu Engineering Laboratory of Light-Electricity-Heat Energy-Converting Materials and Applications, Changzhou University, Changzhou 213164, P. R. China.*

[b] *Department of Chemistry and Hong Kong Branch of Chinese National Engineering Research Center for Tissue Restoration & Reconstruction, Hong Kong University of Science and Technology, Clear Water Bay, Kowloon, Hong Kong*

[c]*College of Chemistry, Key Lab of Environment-Friendly Chemistry and Application in Ministry of Education, Xiangtan University, Xiangtan 411105, China.*

[d] *Hong Kong University of Science and Technology-Shenzhen Research Institute, No. 9 Yuexing first RD, Hi-tech Park, Nanshan, Shenzhen 518057, P. R. China.*

[e]*Department of Physics, Chinese University of Hong Kong, New Territories, Hong Kong, P. R. China.*

‡ These authors contributed equally to this work.

Email addresses:

(T Liu) liutaozhx@ust.hk

(H. Yan) hyan@ust.hk

(Y Liu) liuyu03b@126.com

Contents

Experimental Procedures

1. Materials and Instruments

All reagents and chemicals were purchased commercially and used directly without further purification unless otherwise stated. Anhydrous toluene and tetrahydrofuran (THF) were distilled from Na/benzophenone under argon flow. Unless otherwise stated, all reactions were carried out under inert atmosphere using standard Schlenk-line techniques. Particularly, SM1 and SM2 were synthesized according to the literatures.[1,2] ^{1}H and ^{13}C NMR spectra were recorded on Bruker Ascend 400 MHz spectrometer using $CDCl_3$ as the deuterium solvent. Mass spectra (MS) were measured on a Bruker Daltonics BIFLEX III MALDITOF analyzer. Elemental analyses (EAs) of polymers were characterized by Vario EL III analyses. Polymer molecular weights were evaluated by gel permeation chromatography (GPC) using THF as the eluent and polystyrenes as the standards. UV-vis absorption spectra of polymer solutions and films were recorded on a Shimadzu HP-453 UV spectrophotometer. Cyclic voltammetry (CV) was conducted on a CHI620 voltammetric analyzer under argon atmosphere in an anhydrous acetonitrile solution of tetra(n-butyl) ammonium hexafluorophosphate (Bu_4NPF_6, 0.1 M) at a scan rate of 50 mV/s. A platinum disk working electrode, a platinum wire counter electrode and an Ag/AgCl electrode were used as working electrode, counter electrode, reference electrode, respectively, and the ferrocene/ferrocenium (Fc/Fc^+) redox couple was used as the reference for all measurements with a scanning rate of 50 mV s^{-1}. Thermogravimetric analysis (TGA) was measured on a Perkin-Elmer Diamond

TG/DTA thermal analyzer at a scan rate of 10 °C/min under nitrogen atmosphere. The external quantum efficiency (EQE) spectra of solar cells were recorded by a QE-R3011 measurement system (Enli Technology, Inc.). AFM measurements were obtained by using a Dimension Icon AFM (Bruker) in a tapping mode (2 × 2 μm^2). The grazing incidence X-ray scattering (GIWAXS) measurement was carried out with a Xeuss 2.0 SAXS/WAXS laboratory beamline using a Cu X-ray source (8.05 keV, 1.54 Å) and a Pilatus3R 300K detector. The incident angle was 0.2°. The samples for GIWAXS measurements were fabricated on silicon substrates using the same recipe for the devices. The electron and hole mobility were measured by using the method of space-charge limited current (SCLC) for electron-only devices with the structure of ITO/ZnO/active layer/PNDIT-F3N/Ag and hole-only devices with the structure of ITO/PEDOT:PSS/active layer/MoO_3/Ag The charge carrier mobility was determined by fitting the dark current to the model of a single carrier SCLC according to the equation: $J = 9\varepsilon_0\varepsilon_r\mu V^2/8d^3$, where J is the current density, d is the film thickness of the active layer, μ is the charge carrier mobility, ε_r is the relative dielectric constant of the transport medium, and ε_0 is the permittivity of free space. $V = V_{app} - V_{bi}$, where V_{app} is the applied voltage, V_{bi} is the offset voltage. The carrier mobility can be calculated from the slope of the $J^{1/2} \sim V$ curves.

2. Fabrication and characterization of polymer solar cells

Solar cells were fabricated in a conventional device configuration of ITO/PEDOT:PSS/donors:MeIC/PNDIT-F3N/Ag. The ITO substrates were first scrubbed by detergent and then sonicated with deionized water, acetone and

isopropanol subsequently, and dried overnight in an oven. The glass substrates were treated by UV-Ozone for 30 min before use. PEDOT:PSS (Heraeus Clevios P VP AI 4083) was spin-cast onto the ITO substrates at 4000 rpm for 30 s, and then dried at 150 °C for 15 min in air. The donor: acceptor blends (1.1:1 weight ratio) were dissolved in chloroform (the total concentration of blend solutions was 16.8 mg mL^{-1} for all blends and DIO was chosen as additive whose volume ratio was 0.25%) and stirred overnight in room temperature in a nitrogen-filled glove box. The blend solution was spin-cast at 3000 rpm for 30 s. Active layers were annealed at 95 °C hotplate for 5 minutes after being coated. A thin PNDIT-F3N layer was coated on the active layer, followed by the deposition of Ag (100 nm) (evaporated under 5×10^{-5} Pa through a shadow mask). The optimal active layer thickness measured by a Bruker Dektak XT stylus profilometer was about 105 nm. The current density-voltage (*J-V*) curves of all encapsulated devices were measured using a Keithley 2400 Source Meter in air under AM 1.5G (100 mW cm^{-2}) using a Newport solar simulator. The light intensity was calibrated using a standard Si diode (with KG5 filter, purchased from PV Measurement to bring spectral mismatch to unity). Optical microscope (Olympus BX51) was used to define the device area (5.9 mm^2). EQEs were measured using an Enlitech QE-S EQE system equipped with a standard Si diode. Monochromatic light was generated from a Newport 300W lamp source.

3. Chemical Synthesis

As shown in Scheme S1, both BDTT-Q_X type copolymers, namely PBDTTS-TClQx and PBDTTS-TClSQx, had been synthesized and characterized. The detailed

synthesis procedures of PBDTTS-TClQx and PBDTTS-TClSQx are depicted in Scheme S1. All monomers SM1-SM9, TClQx and TClSQx were synthesized through Williamson reaction, Sonogashira coupling, Still coupling, condensation reaction and so on, with a yield 70%~85% of each step. Finally, then the

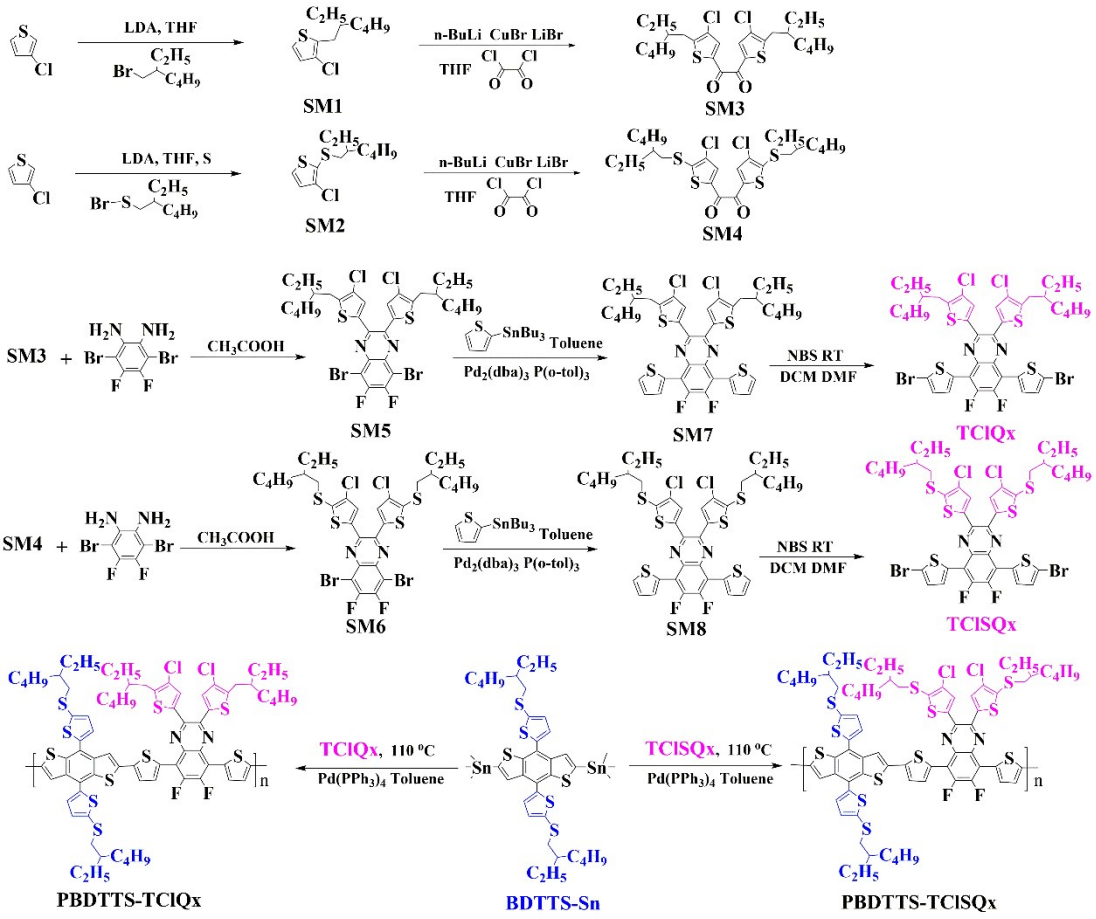

Scheme S1. The synthetic routes of PBDTTS-TClQx and PBDTTS-TClSQx.

typical Stille coupling reaction of BDTTS and monomer TClQx and TClSQx obtained the medium band-gap copolymers of PBDTTS-TClQx and PBDTTS-TClSQx with high yield of over 80% (see the Supporting Information for the reaction conditions and procedures). The afforded copolymers were purified by Soxhlet extraction with methanol, acetone, dichloromethane (DCM) and chloroform (CF), respectively, followed by a fast silica gel column chromatography with chloroform as solvent to

remove the oligomers and other impurities. Both copolymers show good solubility in common organic solvents, such as chloroform (CF), chlorobenzene (CB) and dichlorobenzene (*o*-DCB) at room temperature.

3.1. Synthesis of 1,2-bis(4-chloro-5-(2-ethylhexyl)thiophen-2-yl)ethane-1,2-dione (SM3):

In a 250 mL three-neck round-bottom flask, 3-chloro-2-(2-ethylhexyl) thiophene (SM1) (9.3 g, 40.5 mmol) was dissoloved in anhydrous THF (80 mL), the reaction mixture cooled to -78 ^{o}C under a nitrogen atmosphere. To the above reaction mixture solution, the n-BuLi (22.2 mL, 44.55 mmol, 1.1 eq) was slowly added to the reaction mixture and stirred for 2 h. Then lithium bromide (7.05 g, 81.0 mmol, 2.2 eq) and cuprous bromide (5.79, 40.5 mmol, 1.1 eq) dispersed in 50 mL THF was addeds lowly to the mixture at 0 °C under reflux for 1 h, and then the oxalyl chloride (2.6 g, 20.25 mmol, 0.5 eq) was added and the reaction mixture was stirred for 30 min at 0 ^{o}C and for another 2 h at room temperature. The mixture solution was quenched with deionized water, extracted with dichloromethane (DCM, 25 mL × 3), and The organic extracts were washed with brine and aqueous sodium bicarbonate, then dried over anhydrous $MgSO_4$. Subsequently, the organic solvents were evaporated under vacuum. The residue was purified by column chromatography on silica gel using hexane as the eluent to afford **SM3** as a light yellow viscous liquid (2.3 g, 20%). ^{1}H NMR (400 MHz, $CDCl_3$, TMS), δ (ppm): 7.88 (s, 1H), 2.81 (d, 2H), 1.72 (m, 1H), 1.35 (m , 8H), 0.95-0.85 (m, 6H).

3.2. Synthesis of 1,2-bis(4-chloro-5-((2-ethylhexyl)thio)thiophen-2-yl)ethane -1,2-dione (SM4)：

According to the synthetic process of **SM3**, and using SM2 (10.6 g, 40.5 mmol) instead of SM1, **SM4** (9.27 g, 93.0%) was obtained as dark red solid (6.2 g, 48%). ^{1}H NMR (400 MHz, $CDCl_3$, TMS), δ (ppm): 7.97 (s, 1H), 3.10 (d, 2H), 1.75 (dt, 1H), 1.56-1.33 (m, 8H), 0.94 (m, 6H).

3.3. Synthesis of 5,8-dibromo-2,3-bis(4-chloro-5-(2-ethylhexyl)thiophen-2-yl)-6,7-difluoroquinoxaline (SM5)：

In a 100 mL three-necked flask, the the mixture of 3,6-dibromo-4,5-difluorobenzene-1,2-diamine (1.08 g, 36.0 mmol, 1.0 eq) and **SM3** (1.86 g, 36.0 mmol) in anhydrous acetic acid (40 mL) was stirred at 90 °C overnight under a nitrogen atmosphere. After cooling the solution to room temperature, the reaction mixture was poured into water and extracted with DCM (25 mL × 3). The combined organic layers were then dried over anhydrous MgSO4 and evaporated to remove solvent under vacuum. The residue was purified by column chromatography on silica gel using DCM/petroleum ether (v/v, 1:1=1:9) as the eluent to obtain **SM5** as a yellow solid (2.0 g, 71%). ^{1}H NMR (400 MHz, $CDCl_3$, TMS), δ (ppm): 7.36 (s, 1H), 2.81 (d, J = 7.1 Hz, 2H), 1.73 (dt, J = 12.8, 6.3 Hz, 1H), 1.48-1.27 (m, 8H), 0.98-0.88 (m, 6H). ^{13}C NMR (101 MHz, CDCl3) δ 151.66, 146.34, 146.04, 143.84, 136.72, 135.71, 130.47, 123.56, 101.38, 41.13, 32.81, 32.51, 28.90, 25.87, 23.17, 14.31, 10.86.

3.3 Synthesis of 5,8-dibromo-2,3-bis(4-chloro-5-((2-ethylhexyl)thio)thiophen-2-yl) -6,7-difluoroquinoxaline (SM6)

According to the synthetic process of **SM5**, and using **SM4** (5.79 g, 10.0 mmol) instead of **SM3**, **SM6** was obtained as yellow solid (6.34 g, 75%). ^{1}H NMR (400 MHz, $CDCl_3$, TMS), δ (ppm): 7.46 (s, 1H), 3.04 (d, 2H), 1.68 (m, 1H), 1.57-1.29 (m, 8H), 0.96-0.89 (m, 6H). ^{13}C NMR (101 MHz, CDCl3) δ 152.01, 151.85, 149.94, 144.81, 138.71, 138.02, 135.52, 135.50, 130.45, 127.42, 109.10, 109.04, 109.00, 108.94, 41.83, 39.23, 32.26, 28.79, 25.50, 22.95, 14.12, 10.81.

3.4. Synthesis of 2,3-bis(4-chloro-5-(2-ethylhexyl)thiophen-2-yl)-6,7-difluoro-5,8-di(thiophen-2-yl)quinoxaline (SM7)：

In a 100 mL three-necked flask, the the mixture of SM5 (4.0 g, 5.12 mmol), tributyl(thiophen-2-yl)-stannane(4.0 g, 10.75 mmol), $Pd(dba)_3$ (114.8 mg, 0.10 mmol) and $P(o\text{-}tol)_3$ (126.0 mg, 0.416 mmol）in dry toluene (50 mL) was refluxed for 24 h under a nitrogen atmosphere. After cooling the solution to room temperature, the reaction mixture was poured into water and extracted with DCM (25 mL × 3). The combined organic layers were then dried over anhydrous MgSO4 and evaporated to remove solvent under reduced pressure. The residue was purified by column chromatography on silica gel using DCM/petroleum ether (v/v, 1:1=1:9) as the eluent to obtain **SM7** as orange viscous liquid(3.6 g, 90% yield). ^{1}H NMR (400 MHz, $CDCl_3$, TMS), δ (ppm): 8.01 (d, 1H), 7.68 (d, 1H), 7.38 (s, 1H), 7.29 (s, 1H), 2.84 (d, 2H), 1.75 (m, 1H), 1.50-1.28 (m, 8H), 0.96 (m, 6H). ^{13}C NMR (101 MHz, CDCl3) δ 151.12, 150.52, 147.94, 147.54, 143.57, 143.49, 136.62, 132.98, 132.85, 131.97, 131.84, 131.13, 130.33, 130.14, 130.06, 123.09, 118.89, 117.06, 117.01, 116.46, 116.31, 40.86, 32.44, 32.27, 28.73, 25.75, 23.03, 14.20 , 10.90.

3.5. Synthesis of 2,3-bis(4-chloro-5-((2-ethylhexyl)thio)thiophen-2-yl)-6,7-difluoro -5,8-di(thiophen-2-yl)quinoxaline (SM8)：

According to the synthetic process of **SM7**, and using **SM6** (5.33 g, 5.12 mmol) instead of **SM5**, **SM7** was obtained as an orange-red viscous liquid (4.02 g, 92%). ^{1}H NMR (400 MHz, $CDCl_3$, TMS), δ (ppm): 7.99 (d, 1H), 7.69 (dd, 1H), 7.44 (s, 1H), 7.29 (s, 1H), 3.01 (d, 2H), 1.67 (m, 1H), 1.49-1.28 (m, 8H), 0.93 (m, 6H). ^{13}C NMR (101 MHz, CDCl3) δ 151.00, 150.84, 148.93, 148.78, 142.41,139.86, 139.29, 126.23, 134.35, 131.16, 131.11, 131.06, 130.23, 130.07, 130.04, 128.16, 126.71, 117.78, 114.07, 41.63, 39.22, 32.18, 28.73, 25.42, 22.96, 14.05, 10.83.

3.6. Synthesis of 5,8-bis(5-bromothiophen-2-yl)-2,3-bis(4-chloro-5-(2-ethylhexyl) thiophen-2-yl)-6,7-difluoroquinoxaline (TClQx)：

Under a nitrogen atmosphere, in a 100 mL three-necked flask, the mixture of **SM7** (786.0 mg, 1.0 mmol) and *N*-bromosuccinimide (NBS) (426.0 mg, 2.1 mmol) in dichloromethane (40 mL) and dimethyl formamide (DMF, 20 mL) was stirred for 12 h at room temperature under dark conditions. After cooling the solution to room temperature, the reaction mixture was poured into water and extracted with DCM (25 mL × 3). The combined organic layers were then dried over anhydrous MgSO4 and evaporated to remove solvent under reduced pressure. The residue was purified by column chromatography on silica gel using DCM/petroleum ether (v/v, 1:1=1:10) as the eluent to obtain **TClQx** as a red solid (756.0 mg, 80% yield). ^{1}H NMR (400 MHz, $CDCl_3$, TMS), δ (ppm): 7.76 (d, J = 4.1 Hz, 1H), 7.36 (s, 1H), 7.20 (d, J = 4.2 Hz, 1H), 2.87 (d, J = 5.2 Hz, 2H), 1.85 – 1.74 (m, 1H), 1.55 – 1.31 (m, 8H), 0.99 – 0.93

(m, 6H). ^{13}C NMR (101 MHz, CDCl3) δ 150.89, 150.70, 148.33, 148.12, 143.54, 143.03, 136.07, 133.45, 133.40, 133.36, 131.90, 131.11, 131.03, 130.95, 130.14, 129.35, 123.16, 118.88, 116.83, 116.77, 116.74, 40.93, 32.59, 32.22, 28.89, 25.75, 23.02, 14.16, 10.93. MALDI-MS (m/z) of $C_{40}H_{40}Br_2Cl_2F_2N_2S_4$ for [M^+]: calcd. 945.72; found, 945.04.

3.7. Synthesis of 5,8-bis(5-bromothiophen-2-yl)-2,3-bis(4-chloro-5-((2-ethylhexyl) thio)thiophen -2-yl)-6,7-difluoroquinoxaline (TClSQx):

According to the synthetic process of **TClQx**, and using **SM8** (852.0 mg, 1.0 mmol) instead of **SM7**, **TClSQx** was obtained as dark red solid (825.0 mg, 82%). ^{1}H NMR (400 MHz, $CDCl_3$, TMS), δ (ppm): 7.73 (d, *J* = 3.8 Hz, 1H), 7.43 (s, 1H), 7.19 (d, *J* = 4.1 Hz, 1H), 3.09 (d, *J* = 6.2 Hz, 2H), 1.55 – 1.33 (m, 8H), 0.98-0.90 (m, 6H). ^{13}C NMR (101 MHz, CDCl3) δ 151.01, 150.82, 148.42, 148.23, 142.57, 138.62, 137.76, 133.51, 133.46, 133.42, 131.69, 131.22, 131.14, 131.06, 130.86, 130.46, 129.44, 126.75, 118.85, 116.88, 116.82, 116.79, 41.33, 39.36, 32.10, 28.79, 25.55, 22.87, 14.13, 10.78. MALDI-MS (m/z) of $C_{40}H_{40}Br_2Cl_2F_2N_2S_6$ for [M^+]: calcd. 1009.84; found, 1009.08.

3.8. Synthesis of copolymer PBDTTS-TClQx:

To a 25 mL reaction tube equipped with a stirring bar was added the monomer **TClQx** (141.7 mg, 0.15 mmol, 1eq), the distannylated monomer BDTTS-Sn (159.7 mg, 0.15 mmol, 1eq), $Pd(PPh_3)_4$ (2.78 mg, 0.0015 mmol, 1.5% eq) and anhydrous toluene (6.0 mL). The reaction tube was purged with argon and sealed under argon flow and the tube was heated to 110 °C for 18 h. After cooled to room temperature,

the reaction solution was added dropwise into 80 mL methanol under vigorous stirring and stirred for 1 h, and collected by filtration and successively extracted in Soxhlet apparatus with methanol, acetone, dichloromethane (DCM) and chloroform (CF), respectively. The precipitate was filtrated and purified by a silica gel column ($CHCl_3$) to yield the product polymer as a deep green solid (161.6 mg, 75.3%). ^{1}H NMR (400 MHz, $CDCl_3$, TMS), δ (ppm): 7.74-6.33 (br, 12H), 3.67-2.40 (br, 8H), 2.28-0.34 (br, 60H). Calcd for $C_{74}H_{82}Cl_2F_2N_2S_{10}$: C, 62.20; H, 5.78; N, 1.96, Found: C, 62.14; H, 5.59, N, 1.88. Molecular weight: M_n = 55.3 kDa, PDI = 2.5.

3.9. Synthesis of copolymer PBDTTS-TClSQx:

PBDTTS-TClSQx was prepared according to the synthetic procedure of PBDTTS-TClQx by the reaction among **TClSQx** (151.0 mg, 0.15 mmol, 1.0 eq), the distannylated monomer BDTTS-Sn (159.7 mg, 0.15 mmol, 1eq), $Pd(PPh_3)_4$ (2.78 mg, 0.0015 mmol, 1.5% eq) and anhydrous toluene (6.0 mL). The reaction was stirred for 16 h until the reaction system becomes a viscous state, and the polymer **PBDTTS-TClSQx** was collected as a deep green solid (175.8 mg, 78.4% yield). ^{1}H NMR (400 MHz, $CDCl_3$, TMS), δ (ppm): 7.97- 6.59 (br, 12H), 3.66-2.38 (br, 8H), 2.15-0.33 (br, 60H). Calcd for $C_{75}H_{86}Cl_2F_2N_2S_{12}$: C, 59.69; H, 5.74; N, 1.86, Found: C, 59.56; H, 5.53, N, 1.82. Molecular weight: M_n = 69.0 kDa, PDI = 2.4.

4: TGA, DSC, optical, GIWAXS, electron and Hole Mobilities data

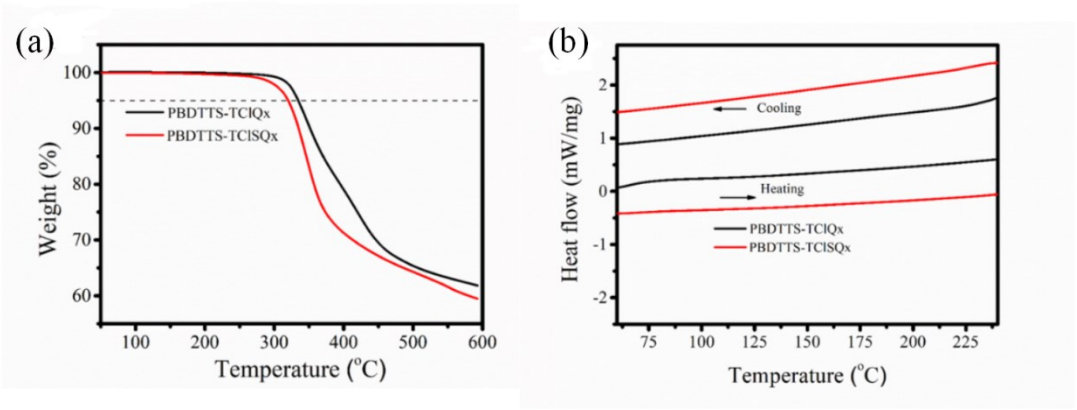

Fig.S1. (a) Thermogravimetric analysis (10 ºC min^{-1}) of copolymers PBDTTS-TClQx and PBDTTS-TClSQx, respectively.

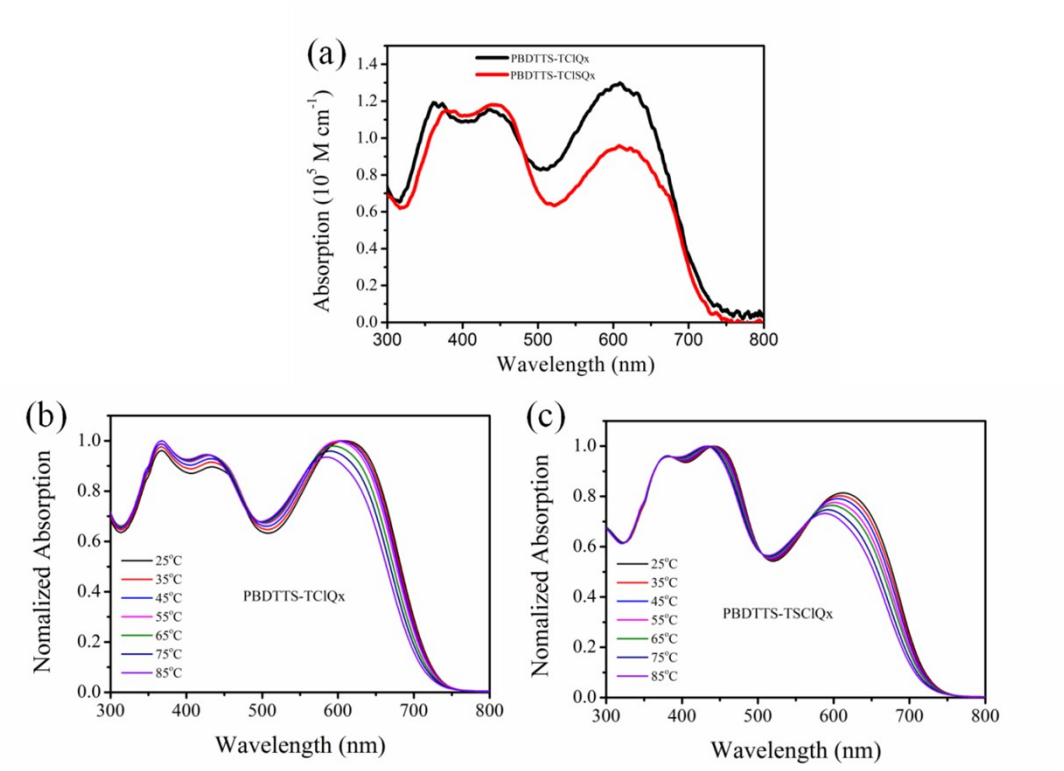

Fig.S2. a) Absorption spectra of PBDTTS-TClQx and PBDTTS-TClSQx in $CHCl_3$ solution; b,c) Temperature-dependent absorption spectra of the these copolymers in dilute chlorobenzene solutions at a temperature interval of 10 °C.

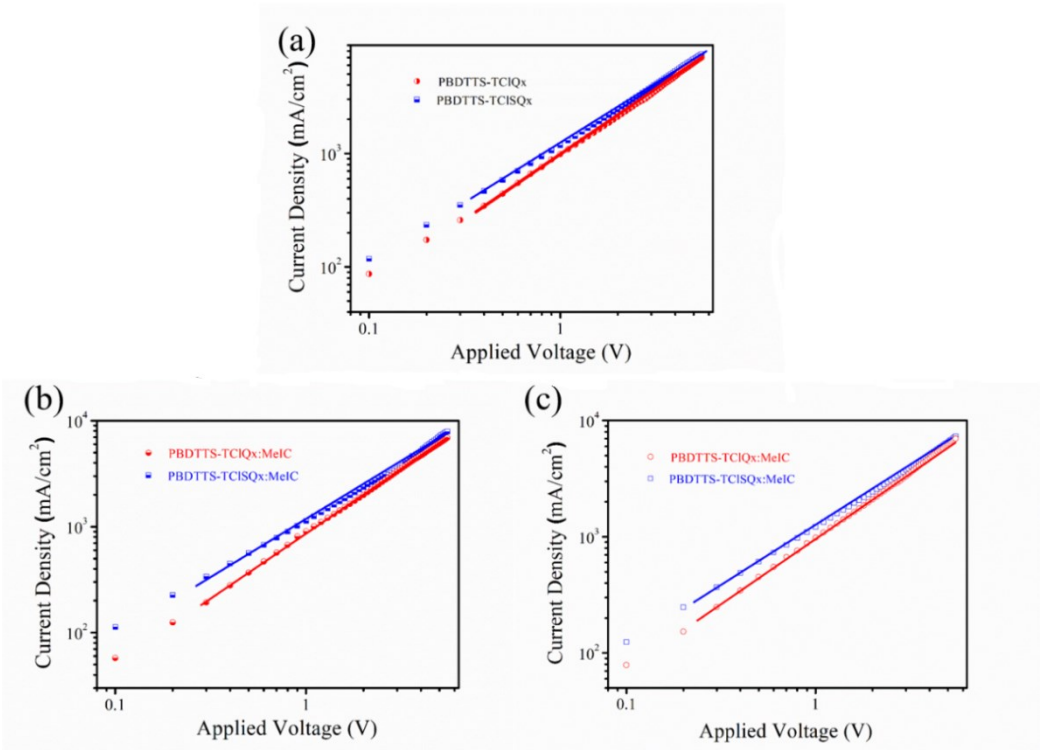

Fig.S3 The *J-V* curves of (a) the hole-only devices with the structure of ITO/MoO_3/copolymers/MoO_3/Al; (b) the hole-only devices with the structure of ITO/MoO_3/copolymers:MeIC/MoO_3/Al and (c) the electron-only devices with the structure of ITO/ZnO/copolymers:MeIC/ZrAcAc/Al according to the SCLC model.

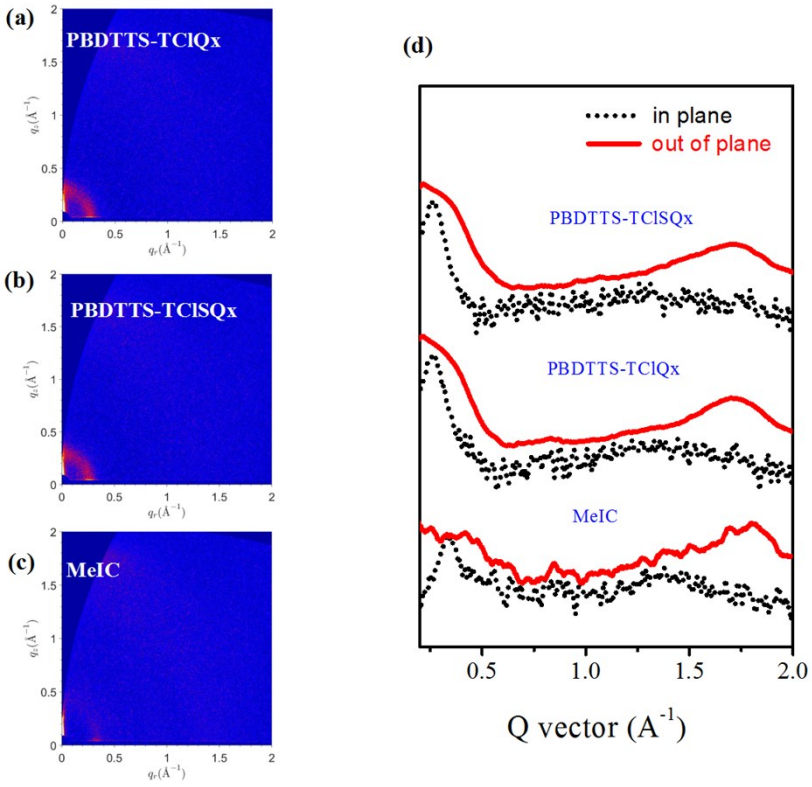

Fig. S4 (a), (b) and (c): Two-dimensional GIWAXS patterns of PBDTTS-TClQx, PBDTTS-TClSQx and MeIC neat films; (d): GIWAXS intensity profiles of PBDTTS-TClQx, PBDTTS-TClSQx and MeIC films along the in-plane (black lines) and out-of-plane (red lines) directions.

Table S1. GIWAXS test performance parameters of the PBDTTS-TClQx (P1), PBDTTS-TClSQx (P2), MeIC, P1:MeIC and P2:MeIC pure films and the related as-cast or thermal annealed blend films.

	in plane			out of plane		
	location ($Å^{-1}$)	d-spacing (Å)	CCL (Å)	location ($Å^{-1}$)	d-spacing (Å)	CCL (Å)
P1	0.26	24.1	56.2	1.70	3.69	19.4
P2	0.25	25.1	46.8	1.72	3.67	15.6
MeIC	0.33	19.0	71.1	1.80	3.49	22.5
P1:MeIC	0.28	22.4	70.3	1.76	3.57	21.2
P2:MeIC	0.28	22.4	56.2	1.79	3.50	16.1

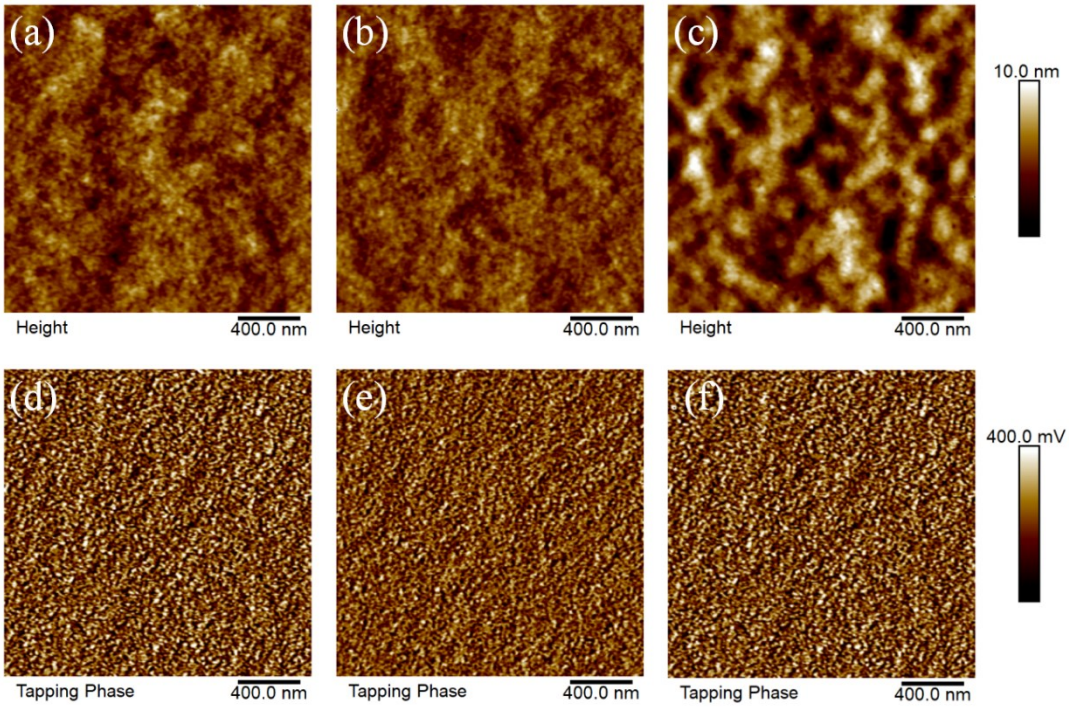

a(c) PBDTTS-TClQx 0.908 nm

b(e) PBDTTS-TClSQx 0.997 nm

c(f) MeIC 1.69 nm

Fig. S5 (a), (b) and (c): AFM height images (Top) and (d), (e) and (f) AFM phase images (Bottom) of PBDTTS-TClQx, PBDTTS-TClSQx and MeIC films.

5. Table S2. NON-PSC photovoltaic performance data based on reported quinoxaline copolymer.

Copolymer Donor:SMA	V_{oc} (V)	J_{sc} (mAcm^{-2})	FF (%)	PCE (%)	Reference
PTQ10:IDTC	0.969	17.81	73.6	12.70	3
PTQ10:Y6	0.87	24.81	75.1	16.21	4
PTQ7:Y6	0.71	18.65	43.4	5.75	4
PTQ8:Y6	0.89	3.11	32.5	0.90	4
PTQ9:Y6	0.82	23.72	54.0	10.50	4
PTQ10:IDTCN	0.98	13.90	54.0	7.40	5
PTQ10:IDTPC	0.93	17.5	74.6	12.2	5
PTQ10:m-ITIC-2F	0.955	18.98	69.1	12.53	6
PTQ10:m-ITIC-4F	0.902	19.76	70.3	12.53	6
PBQ7:Y6	0.81	25.83	60.3	13.45	7
PBQ10:Y6	0.85	25.77	74.6	16.34	7
PBQ-0F:ITIC	0.69	16.16	59.91	6.68	8
PBQ-QF:ITIC	0.83	17.16	62.49	8.90	8
PBQ-4F:ITIC	0.95	17.87	66.80	11.34	8
PBDT-NQx:ITIC	0.87	16.21	64.6	9.11	9
PBDTS-NQx:ITIC	0.92	17.86	69.8	11.47	9
P1:IDIC	0.86	8.53	66.22	4.86	10
P2:IDIC	0.91	13.15	64.84	7.75	10
P3:IDIC	1.00	15.99	60.89	9.70	10
P4:IDIC	1.06	4.82	57.43	2.93	10
PE61:Y6	0.66	23.41	55.30	8.61	11
PE62:Y6	0.78	24.64	62.22	12.02	11
PE63:Y6	0.83	24.68	63.74	13.10	11
PDCB-Q812:ITIC	0.89	10.90	53.30	5.19	12
PDCB-DFQ812:ITIC	1.03	13.44	58.90	8.17	12
PDCB-Q1014:ITIC	0.89	7.98	45.85	3.26	12
PDCB-DFQ1014:ITIC	1.04	10.89	62.30	7.08	12
PNQx-2F2F$_{HW}$:IT-M	0.81	14.10	65.00	7.40	13
PNQx-2F2F$_{LW}$:IT-M	0.80	14.30	66.00	7.50	13
FTQ:ITIC-Th	0.842	16.33	59.60	8.19	14
HFQx:ITIC	0.92	15.60	65.00	9.40	15
HFAQx:ITIC	0.94	15.40	66.00	9.60	16
TTFQx-T1:ITIC	0.90	16.88	69.24	10.52	17
TTFQx-T2:ITIC	0.94	13.75	56.11	7.22	17
HFQx-T:m-ITIC-OR	0.90	16.15	64.00	9.30	18

PffQx-T:ITIC	0.87	16.33	59.6	8.47	19
PffQx-PS:ITIC	0.97	14.96	62.9	9.12	19
DTFFQx-TS:ITIC	0.99	10.40	51.00	5.26	20
ffQx-TS1:ITIC	0.91	13.54	55.00	6.94	21
ffQx-TS2:ITIC	0.91	15.25	56.00	7.69	21
PBDTO-TTFQ:ITIC	0.77	9.60	54.00	3.99	22
PBDTO-TFQ:ITIC	0.88	9.04	44.00	3.49	22
PBDTT-TTFQ:ITIC	0.84	14.06	57.00	6.69	22
PBDTT-TFQ:ITIC	0.95	13.05	57.00	7.06	22
PBDTSi-TTFQ:ITIC	0.95	11.61	57.00	6.21	22
PBDTSi-TTFQ:ITIC	0.92	2.31	35.00	0.75	22
TTFQx-T1:Y5	0.89	21.20	69.60	13.1	23
PTQ10:TPT10	0.92	17.25	58.20	9.24	24
PTQ10:TPT11	0.88	24.79	74.80	16.32	24
PBTOQ:ITIC	0.91	7.99	35.70	2.60	25
PTBOQ-2F:ITIC	0.96	11.88	51.40	5.84	25
PTBTQ-F:ITIT	0.89	7.86	44.00	3.08	25
PTBTQ-2F:ITIC	1.00	5.01	34.40	1.73	25
P(BDTO-TFQ):ITIC	0.88	9.04	44.00	3.49	26
P(BDTT-TFQ):ITIC	0.95	13.05	57.00	7.06	26
P(BDTSi-TFQ):ITIC	0.92	2.31	35.00	0.75	26
PBDTT-QXT-TF1:IDIC	0.95	11.56	60.65	6.67	27
PBDTT-QXT-TF2:IDIC	0.97	9.78	53.61	5.12	27
PTQ10:Y6	0.83	26.65	75.10	16.53	28
PBDTT-TQxT:ITIC	0.84	13.57	65.00	7.39	29
PBDT2FT-TQxT:ITIC	0.98	9.46	53.00	4.90	29
PBDTClT-TQxT:ITIC	0.94	14.61	60.00	8.22	29
PTQ10:Y7	0.85	24.10	69.1	14.2	30
PBDTTS-DTClQx:MeIC	**0.96**	**17.07**	**77.2**	**12.59**	**This Work**
PBDTTS-DTClSQx:MeIC	**0.96**	**15.79**	**73.5**	**11.10**	**This Work**

6: ^{1}H and ^{13}C NMR and Mass Spectra of Compounds

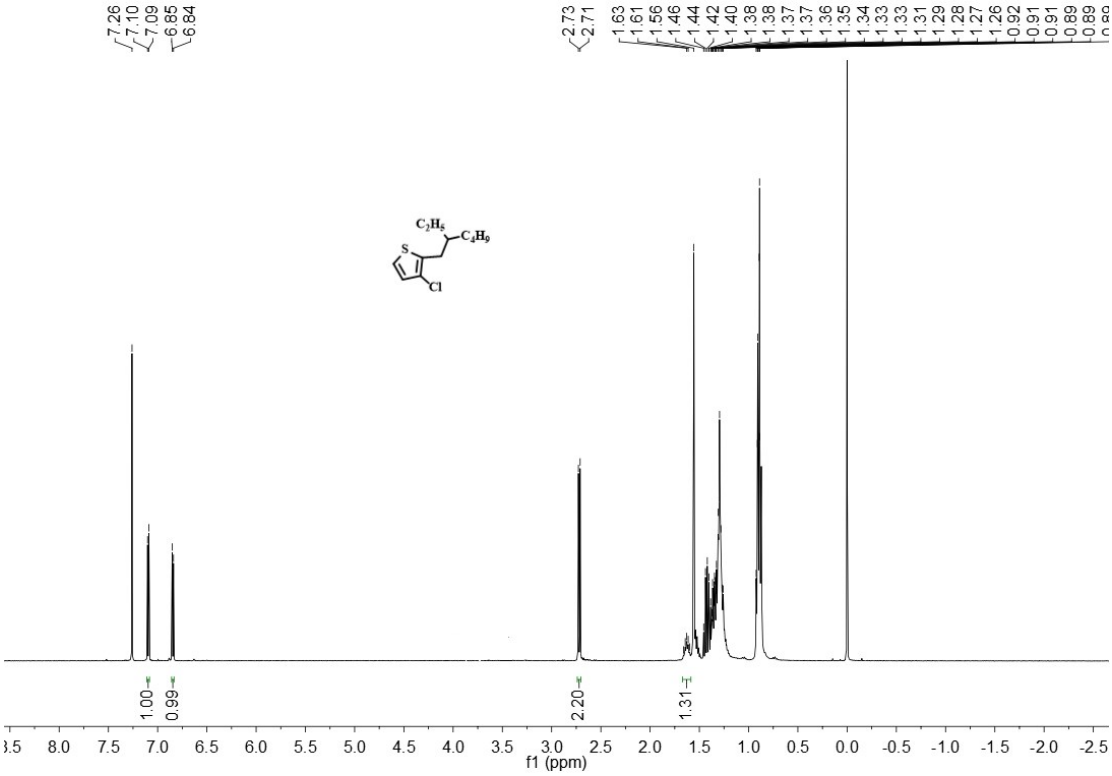

Fig. S7. ^{1}H NMR spectrum of compound SM1 ($CDCl_3$).

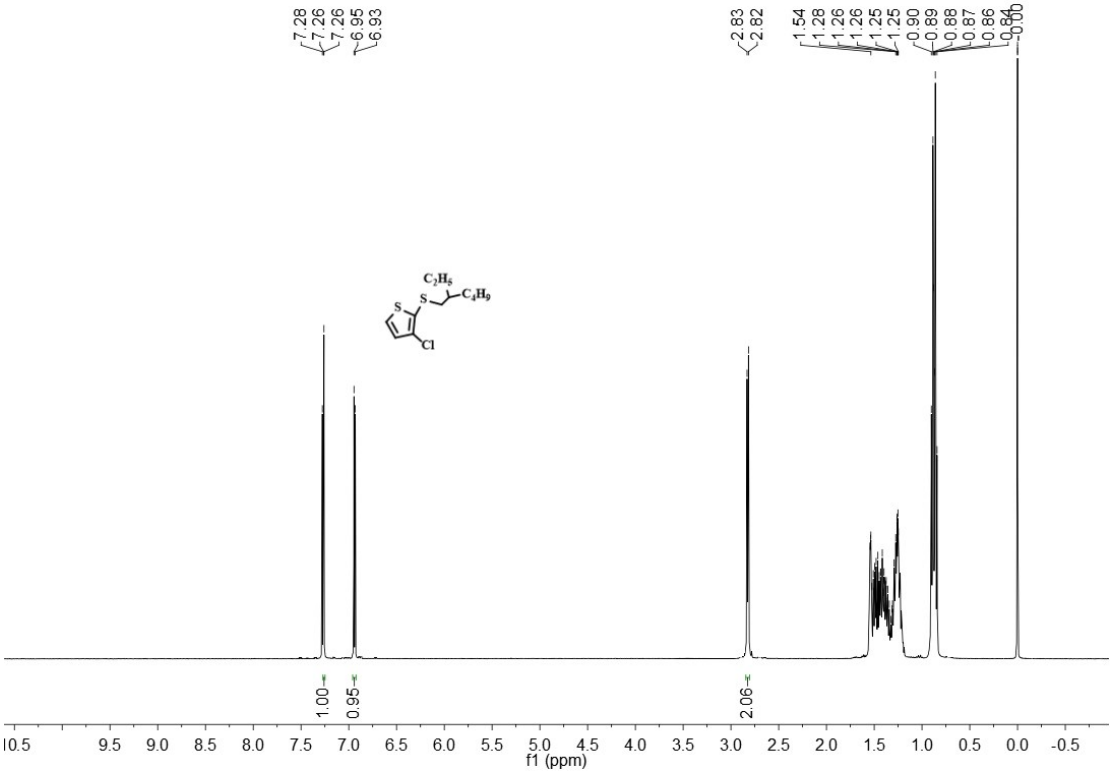

Fig. S8. ^{1}H NMR spectrum of compound SM2 ($CDCl_3$).

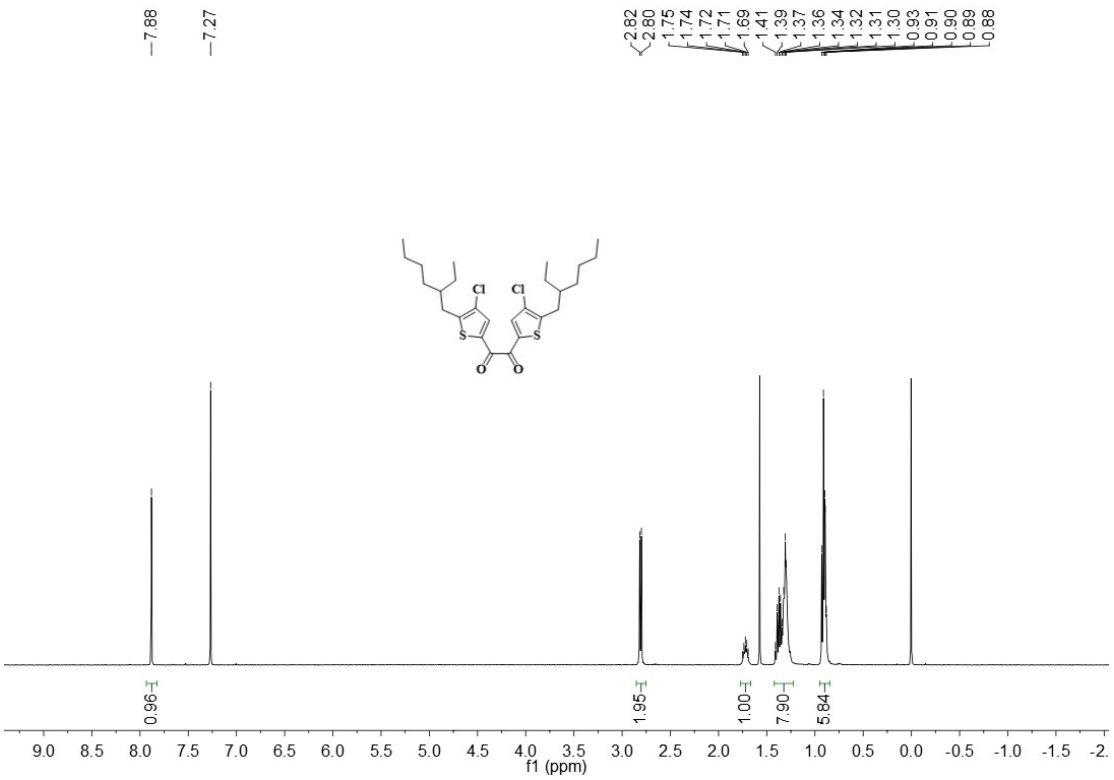

Fig. S9. ^{1}H NMR spectrum of compound SM3 ($CDCl_3$).

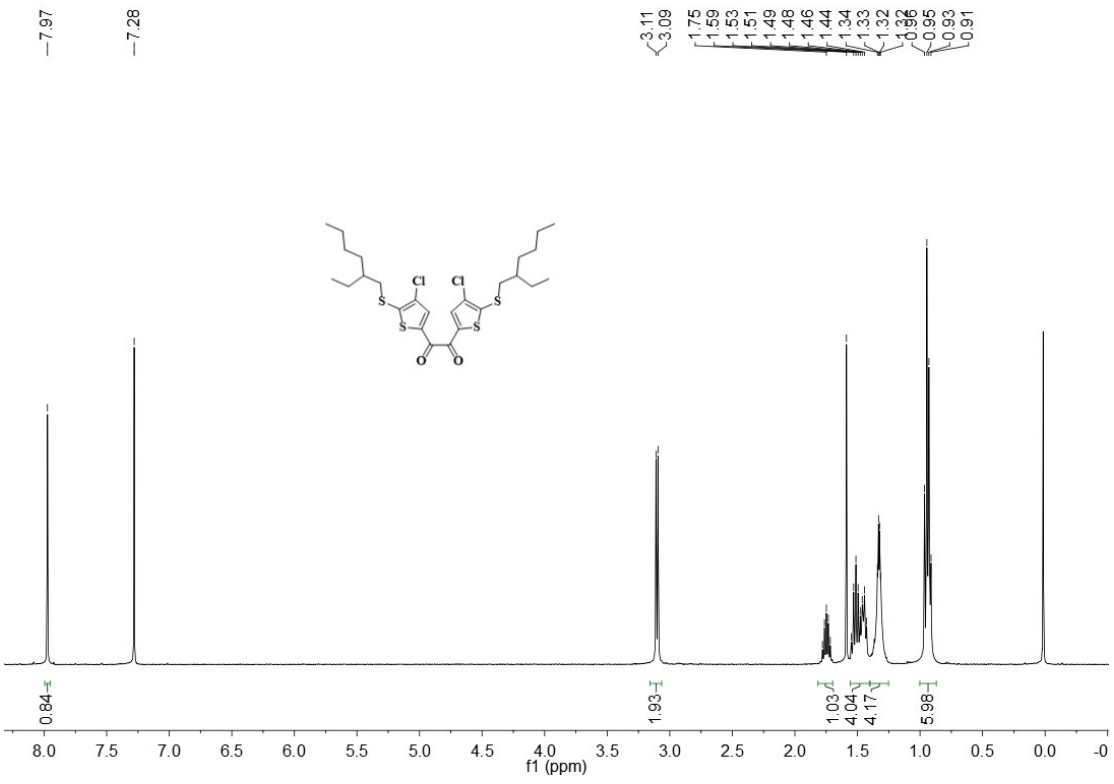

Fig. S10. ^{1}H NMR spectrum of compound SM4 ($CDCl_3$).

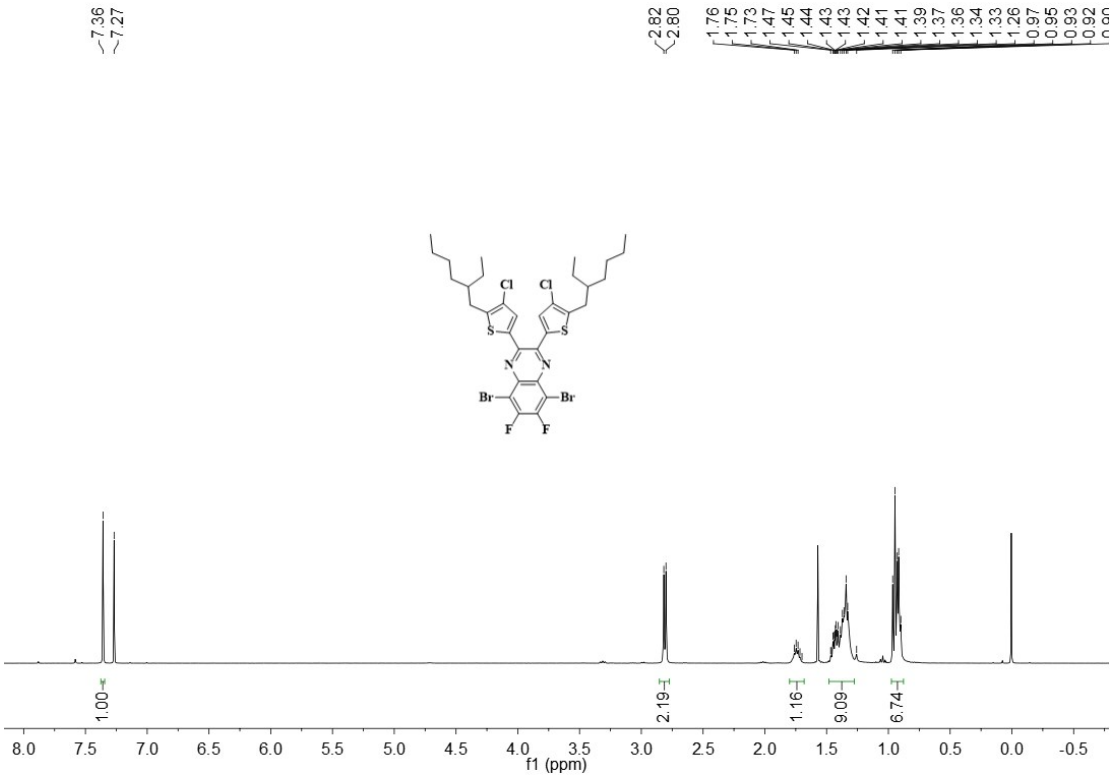

Fig. S11. ^{1}H NMR spectrum of compound SM5 ($CDCl_3$).

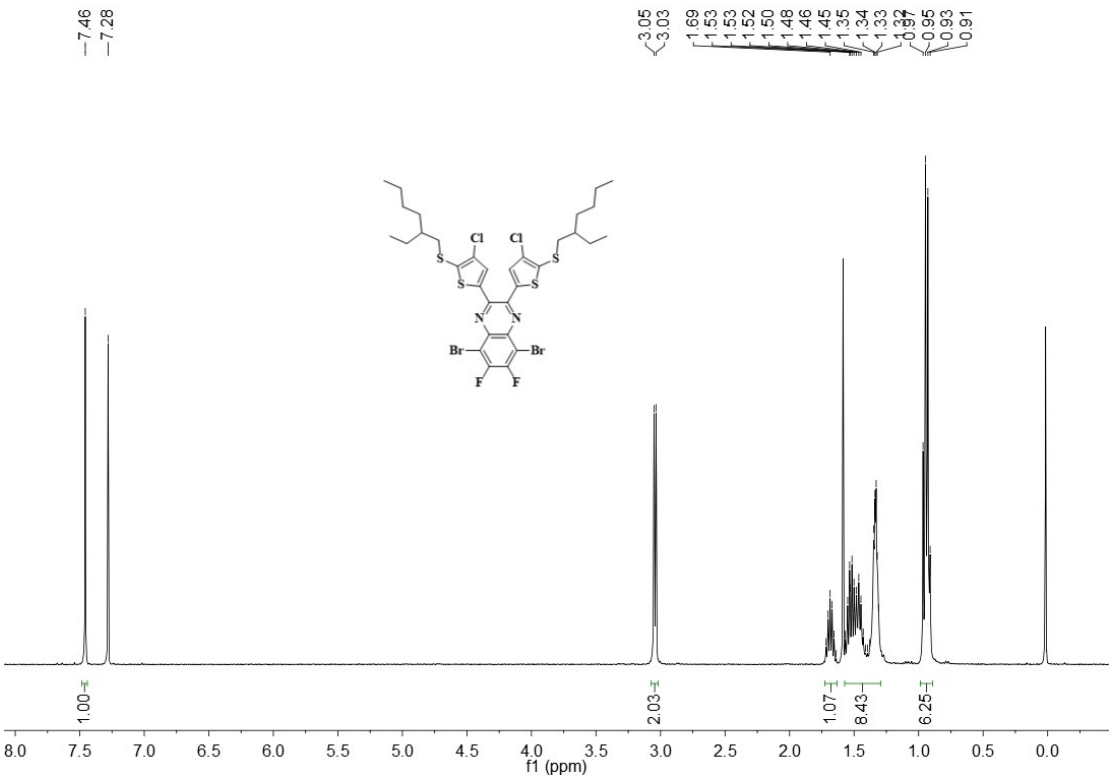

Fig. S12. ^{1}H NMR spectrum of compound SM6 ($CDCl_3$).

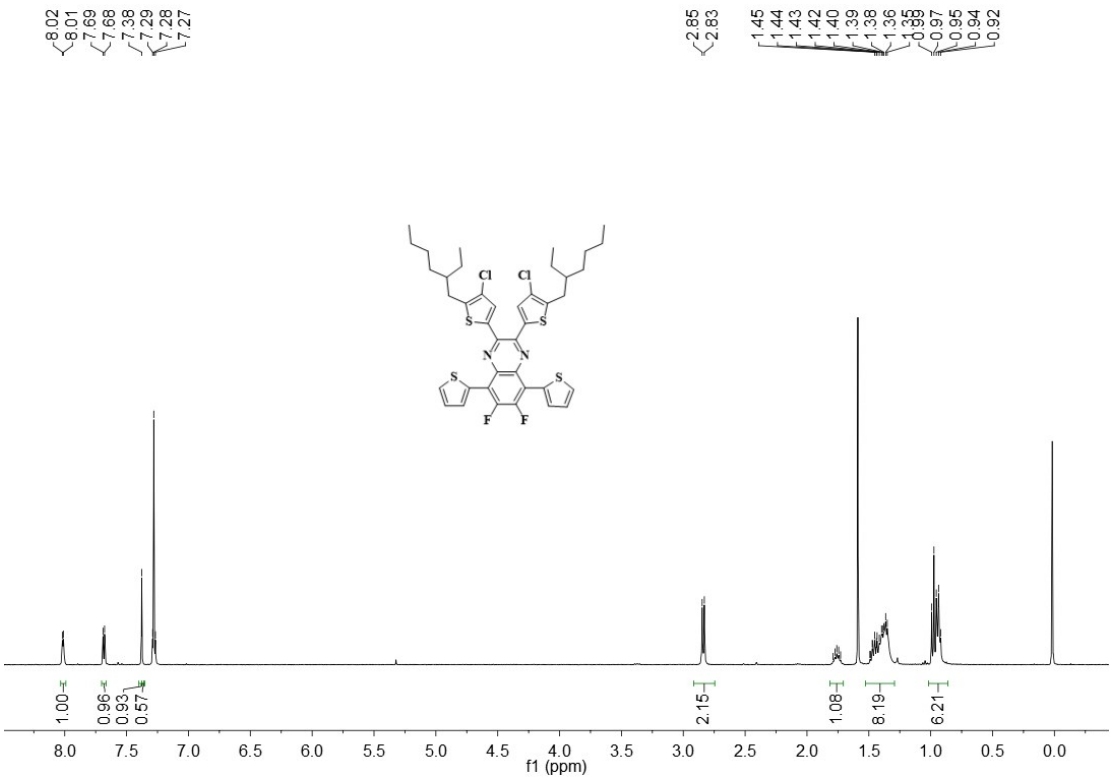

Fig. S13. ^{1}H NMR spectrum of compound SM7 ($CDCl_3$).

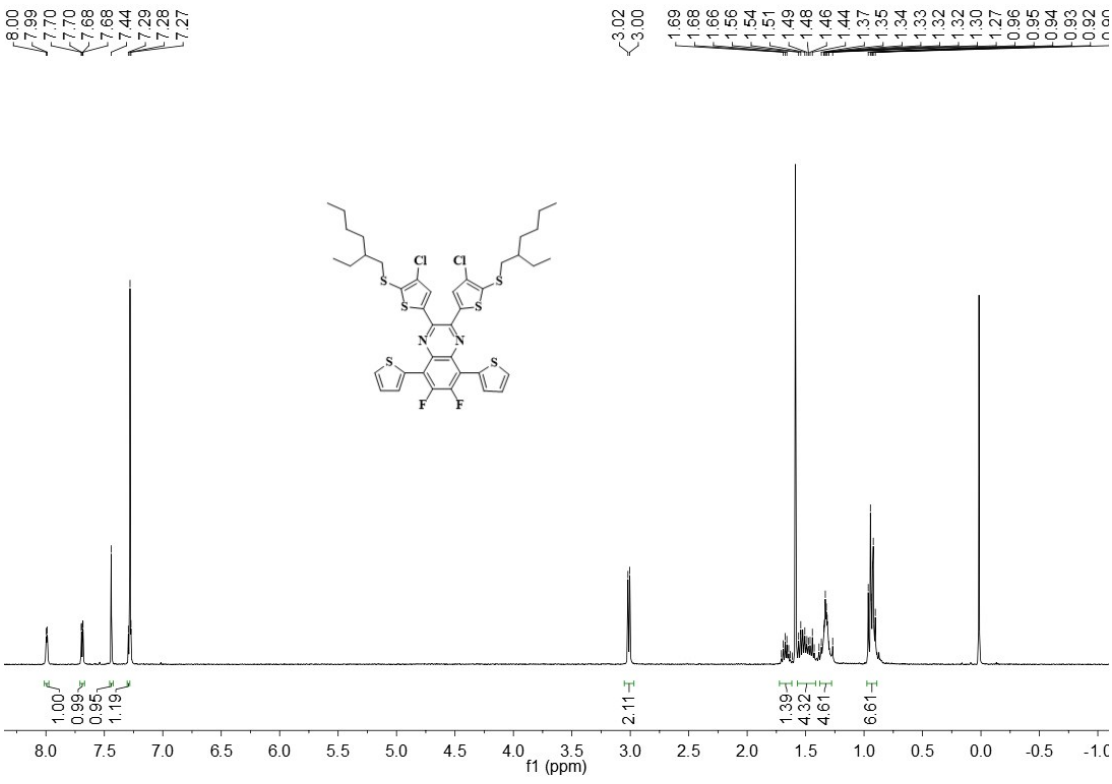

Fig. S14. ^{1}H NMR spectrum of compound SM8 ($CDCl_3$).

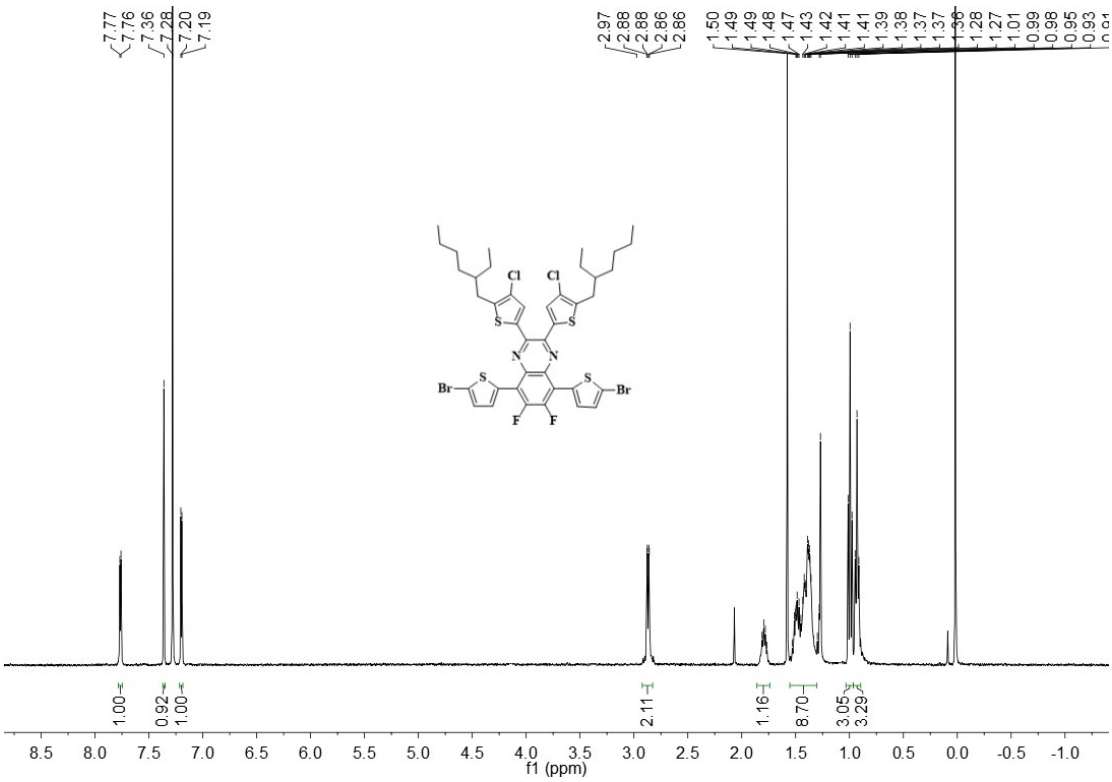

Fig. S15. ^{1}H NMR spectrum of compound TClQx ($CDCl_3$).

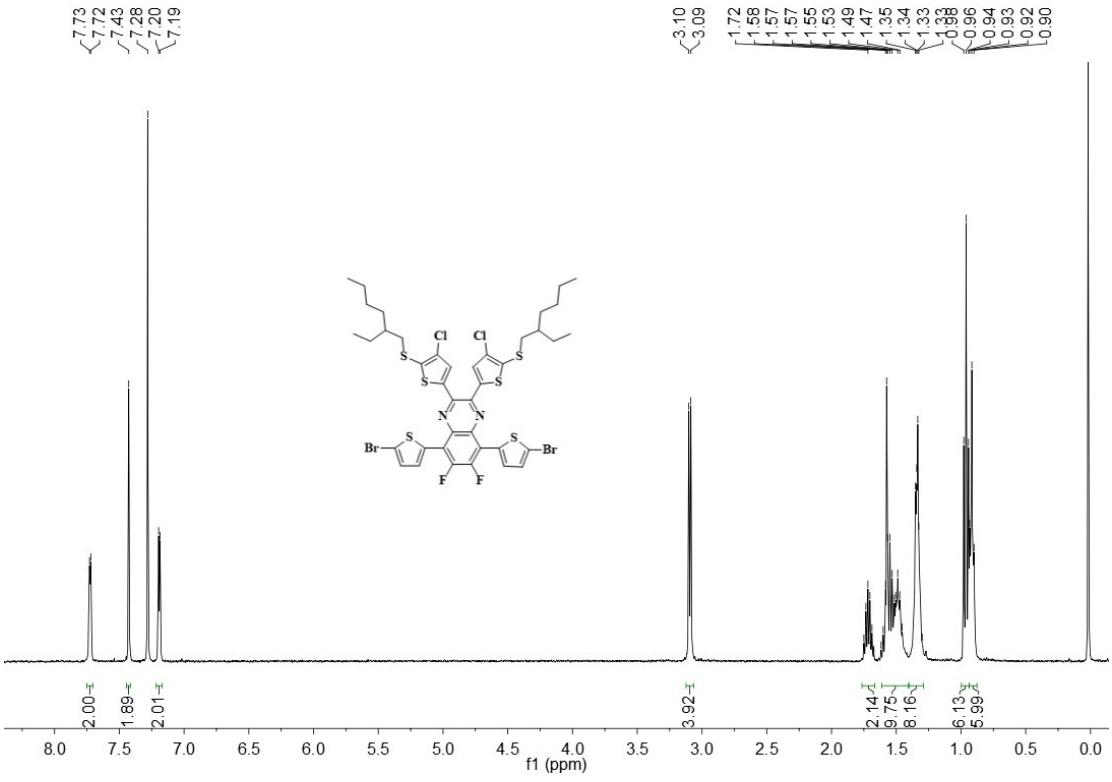

Fig. S16. ^{1}H NMR spectrum of compound TClSQx ($CDCl_3$).

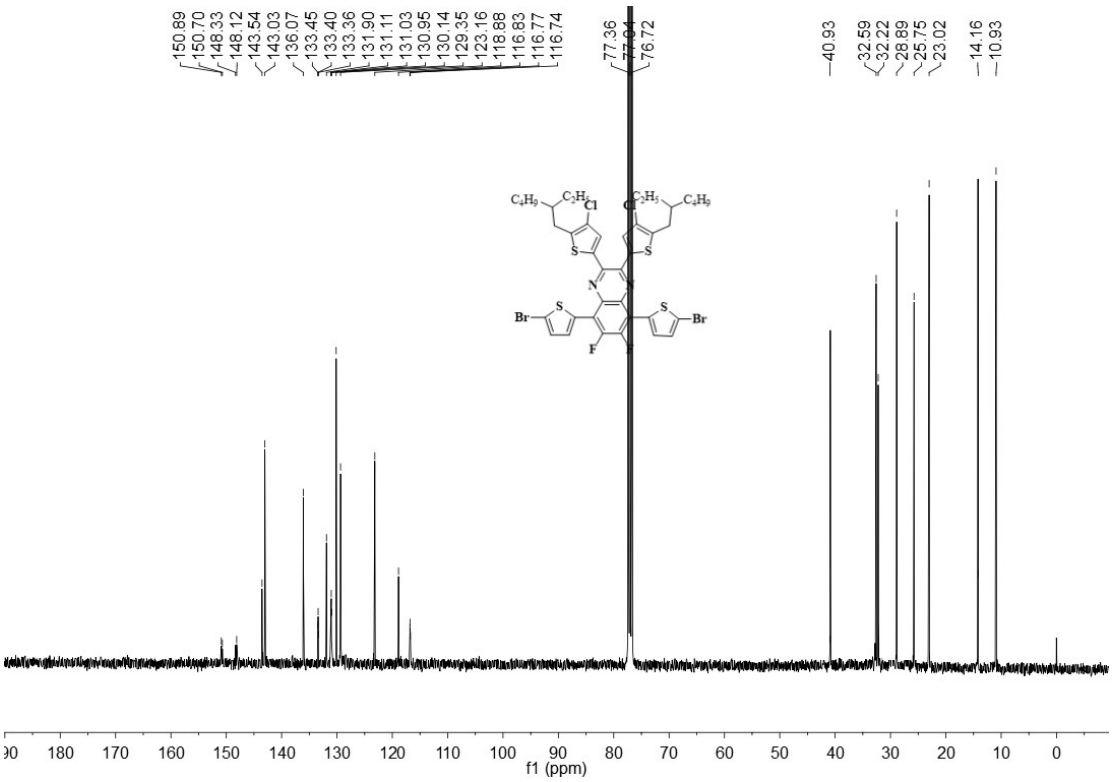

Fig. S17. ^{13}C NMR spectrum of compound TClQx ($CDCl_3$).

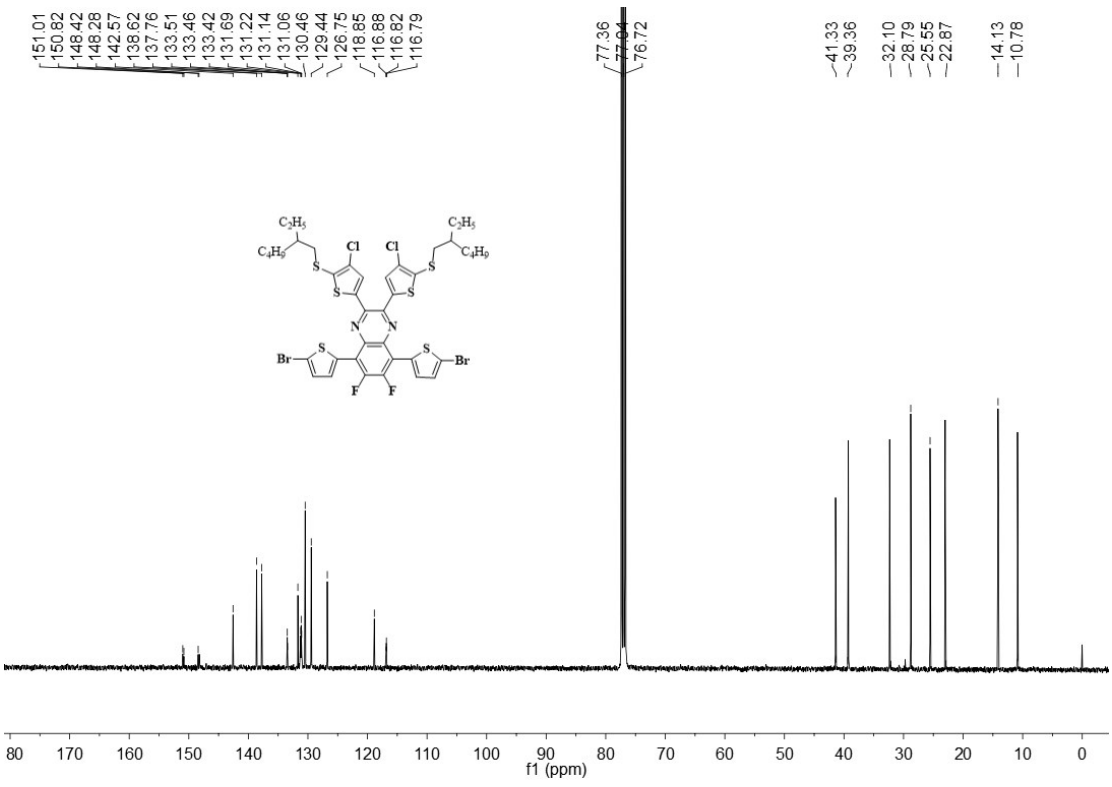

Fig. S18. ^{13}C NMR spectrum of compound TClSQx ($CDCl_3$).

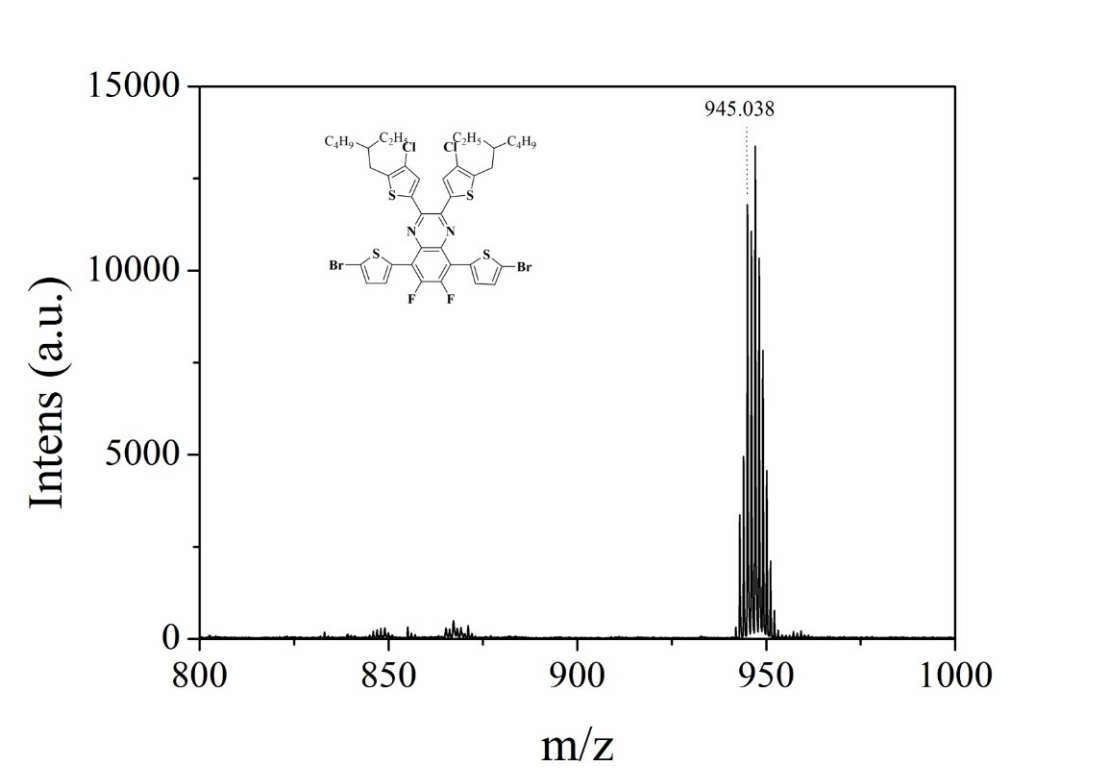

Fig. S19. MALDI-TOF MS spectrum of compound TClQx.

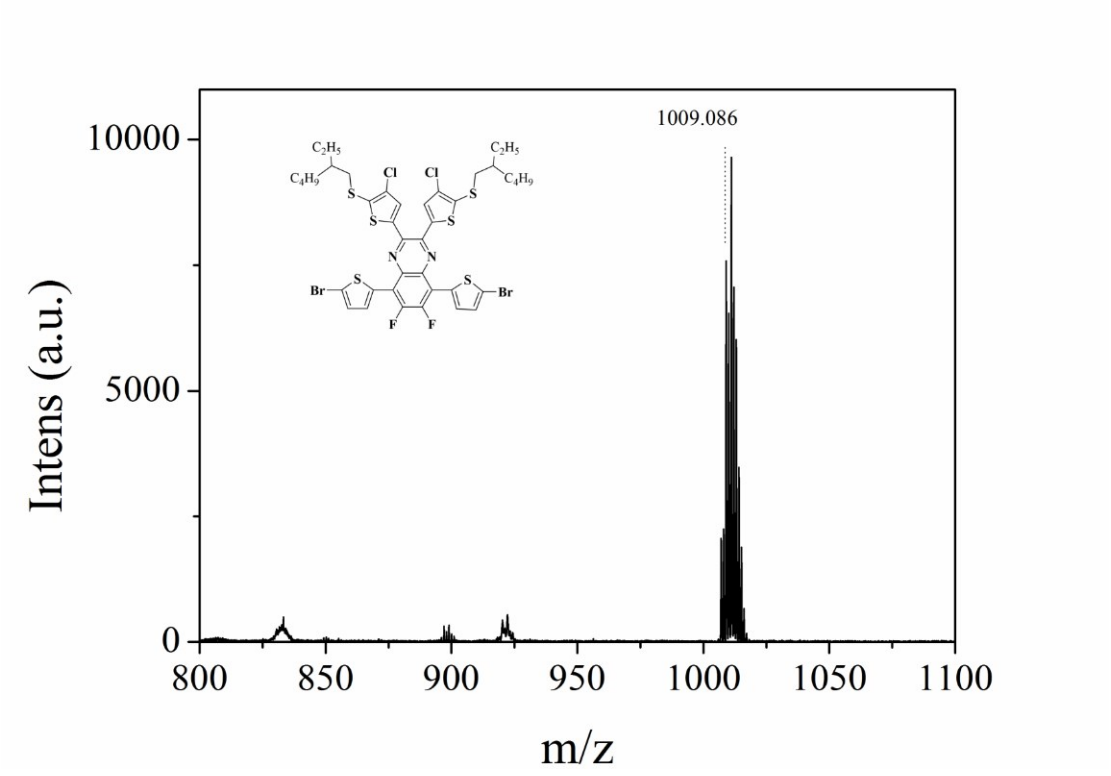

Fig. S20. MALDI-TOF MS spectrum of compound TClSQx.

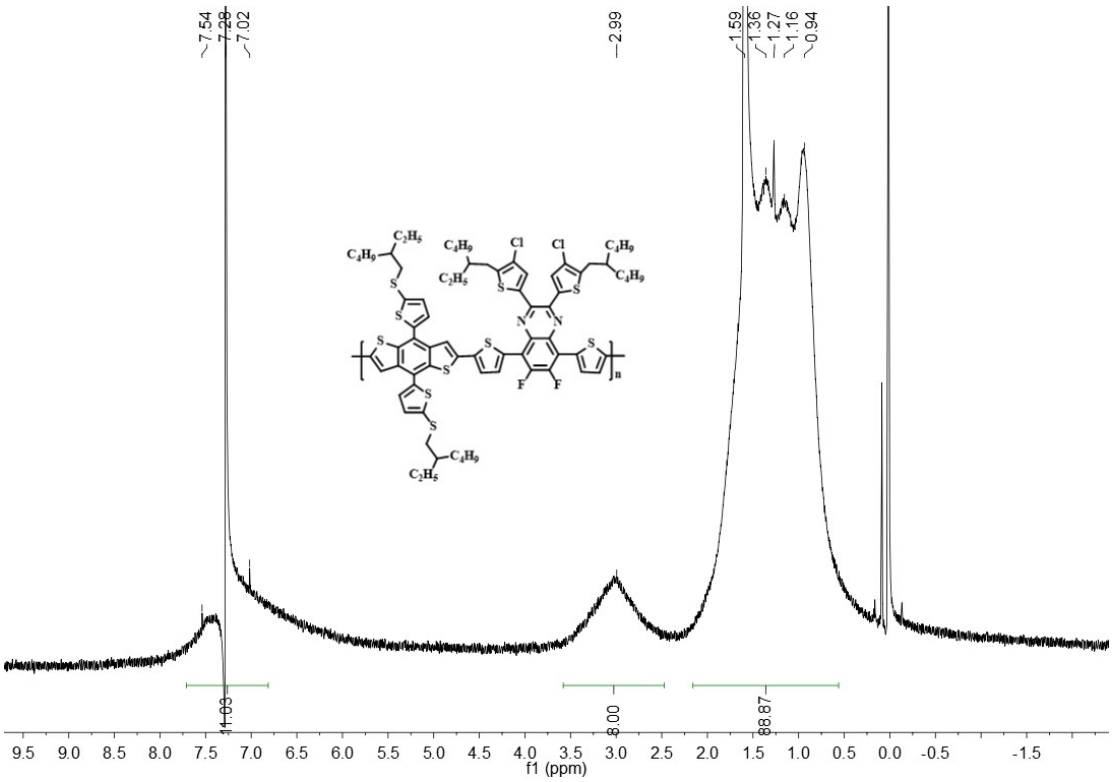

Fig. S21. ^{1}H NMR spectrum of polymer PBDTTS-TClQx ($CDCl_3$).

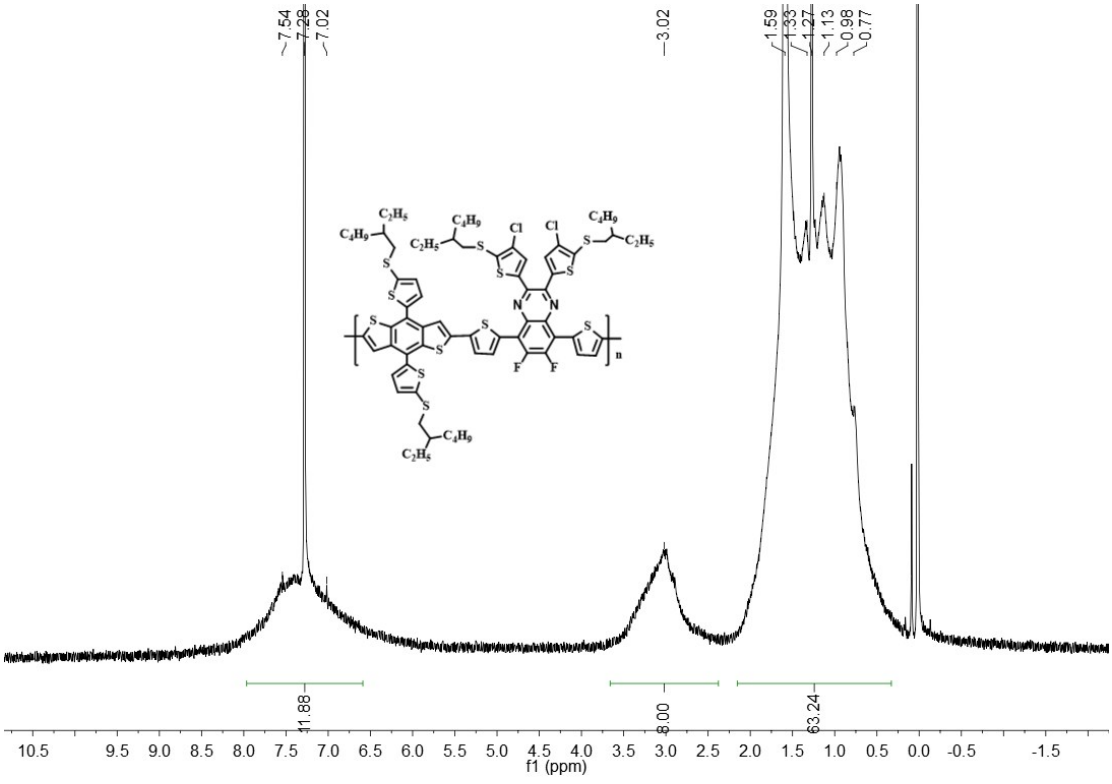

Fig. S22. ^{1}H NMR spectrum of polymer PBDTTS-TClSQx ($CDCl_3$).

References

[1] S. Zhang, Y. Qin, J. Zhu, J. Hou, Over 14% Efficiency in Polymer Solar Cells Enabled by a Chlorinated Polymer Donor, *Adv Mater.*, 2018, **30**, 1800868.

[2] S. Park, H. Ahn, J. Y. Kim, J. B. Park, J. Kim, S. H. Im, H. J. Son, High-Performance and Stable Nonfullerene Acceptor-Based Organic Solar Cells for Indoor to Outdoor Light, *ACS Energy Lett.*, 2019, **5**, 170-179.

[3] C. Sun, F. Pan, H. Bin, J. Zhang, L. Xue, B. Qiu, Z. Wei, Z. G. Zhang, Y. Li, A Low Cost and High Performance Polymer Donor Material for Polymer Solar Cells, *Nat. Commun.*, 2018, **9**, 743.

[4] C. Sun, F. Pan, S. Chen, R. Wang, R. Sun, Z. Shang, B. Qiu, J. Min, M. Lv, L. Meng, C. Zhang, M. Xiao, C. Yang, Y. Li, Achieving Fast Charge Separation and Low Nonradiative Recombination Loss by Rational Fluorination for High-Efficiency Polymer Solar Cells, *Adv Mater.*, 2019, **31**, e1905480.

[5] Z. Luo, C. Sun, S. Chen, Z. G. Zhang, K. Wu, B. Qiu, C. Yang, Y. Li, C. Yang, Side-Chain Impact on Molecular Orientation of Organic Semiconductor Acceptors: High Performance Nonfullerene Polymer Solar Cells with Thick Active Layer over 400 nm, *Adv. Energy Mater.*, 2018, **8**. 1800856.

[6] X. Li, J. Yao, I. Angunawela, C. Sun, L. Xue, A. Liebman-Pelaez, C. Zhu, C. Yang, Z. G. Zhang, H. Ade, Y. Li, Improvement of Photovoltaic Performance of Polymer Solar Cells by Rational Molecular Optimization of Organic Molecule Acceptors, *Adv. Energy Mater.*, 2018, **8**, 1800815.

[7] C. Sun, F. Pan, B. Qiu, S. Qin, S. Chen, Z. Shang, L. Meng, C. Yang, Y. Li, D-A Copolymer Donor Based on Bithienyl Benzodithiophene D-Unit and Monoalkoxy Bifluoroquinoxaline A-Unit for High-Performance Polymer Solar Cells, *Chem. Mater.*, 2020, **32**, 3254-3261.

[8] Z. Zheng, O. M. Awartani, B. Gautam, D. Liu, Y. Qin, W. Li, A. Bataller, K. Gundogdu, H. Ade, J. Hou, Efficient Charge Transfer and Fine-Tuned Energy Level Alignment in a THF-Processed Fullerene-Free Organic Solar Cell with 11.3% Efficiency, *Adv Mater.*, 2017, **29**, 1604241.

[9] T. Yu, X. Xu, G. Zhang, J. Wan, Y. Li, Q. Peng, Wide Bandgap Copolymers Based on Quinoxalino[6,5-f].quinoxaline for Highly Efficient Nonfullerene Polymer Solar Cells, *Adv. Func. Mater.*, 2017, **27**, 1701491.

[10] J. Yang, M. A. Uddin, Y. Tang, Y. Wang, Y. Wang, H. Su, R. Gao, Z. K. Chen, J. Dai, H. Y. Woo, X. Guo, Quinoxaline-Based Wide Band Gap Polymers for Efficient Nonfullerene Organic Solar Cells with Large Open-Circuit Voltages, *ACS Appl. Mater. Interfaces*, 2018, **10**, 23235-23246.

[11] J. Yang, P. Cong, L. Chen, X. Wang, J. Li, A. Tang, B. Zhang, Y. Geng, E. Zhou, Introducing Fluorine and Sulfur Atoms into Quinoxaline-Based p-type Polymers To Gradually Improve the Performance of Fullerene-Free Organic Solar Cells, *ACS Macro Lett.*, 2019, **8**, 743-748.

[12] B. He, Q. Yin, X. Yang, L. Liu, X.-F. Jiang, J. Zhang, F. Huang, Y. Cao, Non-Fullerene Polymer Solar Cells with V_{OC} > 1 V Based on Fluorinated Quinoxaline Unit Conjugated Polymers, *J. Mater. Chem. C*, 2017, **5**, 8774-8781.

[13] S. Pang, L. Liu, X. Sun, S. Dong, Z. Wang, R. Zhang, Y. Guo, W. Li, N. Zheng, C. Duan, F. Huang, Y. Cao, A Wide-Bandgap Conjugated Polymer Based on Quinoxalino[6,5-f]quinoxaline for Fullerene and Non-Fullerene Polymer Solar Cells, *Macromol Rapid Commun.*, 2019, **40**, 1900120.

[14] L. Yang, B. Zhao, H. Wu, J. Liu, H. Liu, J. Wang, W. Wang, Z. Cong, C. Gao, High Lying Energy of Charge-Transfer States and Small Energetic Offsets Enabled by Fluorinated Quinoxaline-Based Alternating Polymer and Alkyl-

Thienyl Side-Chain Modified Non-Fullerene Acceptor, *Org. Electron.*, 2019, **66**, 63-69.

[15] S. Xu, L. Feng, J. Yuan, Z. G. Zhang, Y. Li, H. Peng, Y. Zou, Hexafluoroquinoxaline Based Polymer for Nonfullerene Solar Cells Reaching 9.4% Efficiency, *ACS Appl. Mater. Interfaces*, 2017, **9**, 18816-18825.

[16] T. Wang, T.-K. Lau, X. Lu, J. Yuan, L. Feng, L. Jiang, W. Deng, H. Peng, Y. Li, Y. Zou, A Medium Bandgap D-A Copolymer Based on 4-Alkyl-3,5-difluorophenyl Substituted Quinoxaline Unit for High Performance Solar Cells, *Macromolecules*, 2018, **51**, 2838-2846.

[17] S. Xu, X. Wang, L. Feng, Z. He, H. Peng, V. Cimrová, J. Yuan, Z.-G. Zhang, Y. Li, Y. Zou, Optimizing the Conjugated Side Chains of Quinoxaline Based Polymers for Nonfullerene Solar Cells with 10.5% Efficiency, *J. Mater. Chem. A*, 2018, **6**, 3074-3083.

[18] Z. Zhang, L. Feng, S. Xu, Y. Liu, H. Peng, Z. G. Zhang, Y. Li, Y. Zou, A New Electron Acceptor with meta-Alkoxyphenyl Side Chain for Fullerene-Free Polymer Solar Cells with 9.3% Efficiency, *Adv. Sci.*, 2017, **4**, 1700152.

[19] J. Yuan, L. Qiu, Z.-G. Zhang, Y. Li, Y. Chen, Y. Zou, Tetrafluoroquinoxaline Based Polymers for Non-Fullerene Polymer Solar Cells with Efficiency over 9%, *Nano Energy*, 2016, **30**, 312-320.

[20] F. Cai, L. Li, C. Zhu, J. Li, H. Peng, Y. Zou, Synthesis and Photovoltaic Properties of Alkylthiothiophene Modified Benzodithiophene Polymer, *Chem. Phys. Lett*., 2019, **730**, 271-276.

[21] L. Li, L. Feng, J. Yuan, H. Peng, Y. Zou, Y. Li, Fine-Tuning Blend Morphology via Alkylthio Side Chain Engineering Towards High Performance Non-Fullerene Polymer Solar Cells, *Chem. Phys. Lett.*, 2018, **696**, 19-25.

[22] V. Tamilavan, S. Jang, J. Lee, R. Agneeswari, J. H. Kwon, J. H. Kim, Y. Jin, S. H. Park, Enhanced Photovoltaic Performance of Benzodithiophene-alt-bis (thiophen-2-yl)quinoxaline Polymers via π–Bridge Engineering for Non-Fullerene Organic Solar Cells, *Polymer*, 2020, **194**, 122408.

[23] J. Yuan, Y. Zhang, L. Zhou, C. Zhang, T. K. Lau, G. Zhang, X. Lu, H. L. Yip, S. K. So, S. Beaupre, M. Mainville, P. A. Johnson, M. Leclerc, H. Chen, H. Peng, Y. Li, Y. Zou, Fused Benzothiadiazole: A Building Block for n-Type Organic Acceptor to Achieve High-Performance Organic Solar Cells, *Adv. Mater.*, 2019, **31**, 1807577.

[24] C. Sun, S. Qin, R. Wang, S. Chen, F. Pan, B. Qiu, Z. Shang, L. Meng, C. Zhang, M. Xiao, C. Yang, Y. Li, High Efficiency Polymer Solar Cells with Efficient Hole Transfer at Zero Highest Occupied Molecular Orbital Offset between Methylated Polymer Donor and Brominated Acceptor, *J, Am, Chem, Soc,*, 2020, **142**, 1465-1474.

[25] L. Wang, H. Liu, Z. Huai, Y. Li, S. Yang, Tailoring the Second Acceptor Unit in Easily Synthesized Ternary Copolymers Toward Efficient Non-Fullerene Polymer Solar Cells, *Dyes and Pigments*, 2018, **148**, 72-80.

[26] V. Tamilavan, J. Lee, J. H. Kwon, S. Jang, I. Shin, R. Agneeswari, J. H. Jung, Y. Jin, S. H. Park, Side-Chain Influences on the Properties of Benzodithiophene- alt-di(thiophen-2-yl)quinoxaline Polymers for Fullerene-Free Organic Solar Cells, *Polymer*, 2019, **172**, 305-311.

[27] Y. Zhang, P. Zhou, J. Wang, X. Zhan, X. Chen, Designing a Thiophene-Fused Quinoxaline Unit to Build D–A Copolymers for Non-Fullerene Organic Solar Cells, *Dyes and Pigments*, 2020, **174**, 108022.

[28] Y. Wu, Y. Zheng, H. Yang, C. Sun, Y. Dong, C. Cui, H. Yan, Y. Li, Rationally Pairing Photoactive Materials for High-Performance Polymer Solar Cells with Efficiency of 16.53%, *Sci. China Chem*., 2019, **63**, 265-271.

[29] R. Lenaerts, D. Devisscher, G. Pirotte, S. Gielen, S. Mertens, T. Cardeynaels, B. Champagne, L. Lutsen, D. Vanderzande, P. Adriaensens, P. Verstappen, K. Vandewal, W. Maes, The Effect of Halogenation on PBDTT-TQxT Based Non-Fullerene Polymer Solar Cells-Chlorination vs Fluorination, *Dyes and Pigments*, 2020, **181**,108577.

[30] H. C. Wang, C. H. Chen, R. H. Li, Y. C. Lin, C. S. Tsao, B. Chang, S. Tan, Y. Yang, K. H. Wei, Engineering the Core Units of Small-Molecule Acceptors to Enhance the Performance of Organic Photovoltaics, *Solar RRL*, 2020, DOI: 10.1002/solr.202000253.